Supporting Information

Wet-Chemical Synthesis of Porous Multifaceted Platinum Nanoparticles for Oxygen Reduction and Methanol Oxidation Reactions

Mario Daka,[a] *Marcello Ferrara,*[a] *Manuela Bevilacqua,*[b c] *Paolo Pengo,*[a] *Piu Rajak,*[d] *Regina Ciancio,*[d] *Tiziano Montini,*[a] *Lucia Pasquato*[a] *and Paolo Fornasiero*[a b]*.**

[a] Department of Chemical and Pharmaceutical Sciences, CENMAT, Center of Excellence for Nanostructured Materials, INSTM, UdR Trieste, University of Trieste, Trieste 34127, Italy.

[b] ICCOM-CNR Trieste Research Unit, University of Trieste, Trieste 34127, Italy.

[c] ICCOM-CNR, via Madonna del Piano 10, 50019 Sesto Fiorentino, Italy.

[d] CNR-IOM, TASC Laboratory in Area Science Park, 34139 Trieste, Italy.

* Corresponding author: Paolo Fornasiero, e-mail: pfornasiero@units.it

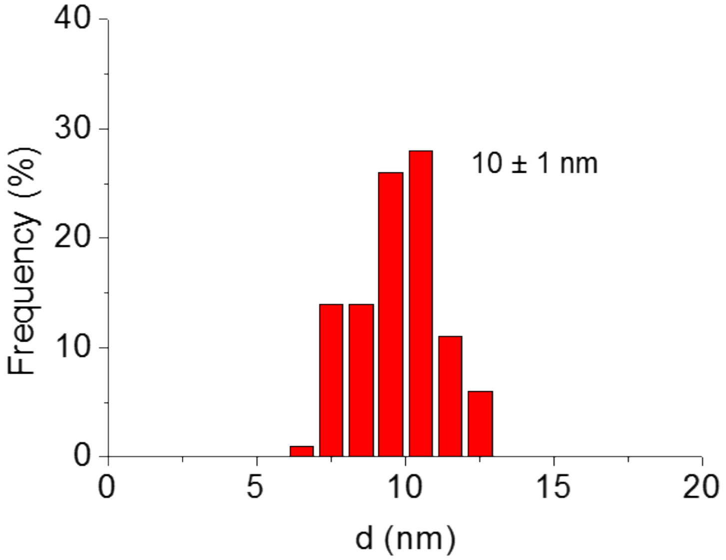

Figure S1. Dimensional analysis of the crystallites constituting the porous Pt NPs.

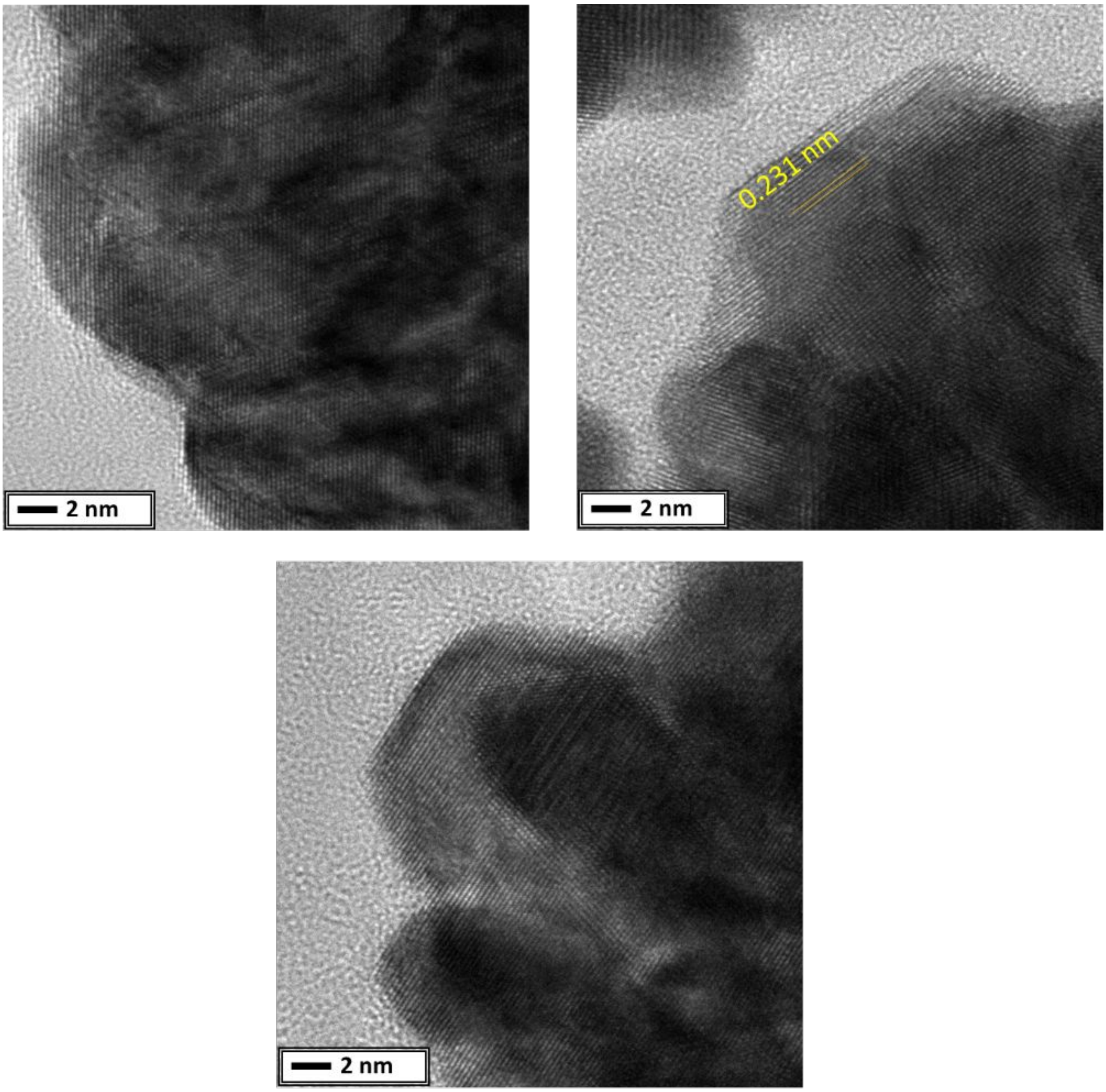

Figure S2. Additional HR-TEM images.

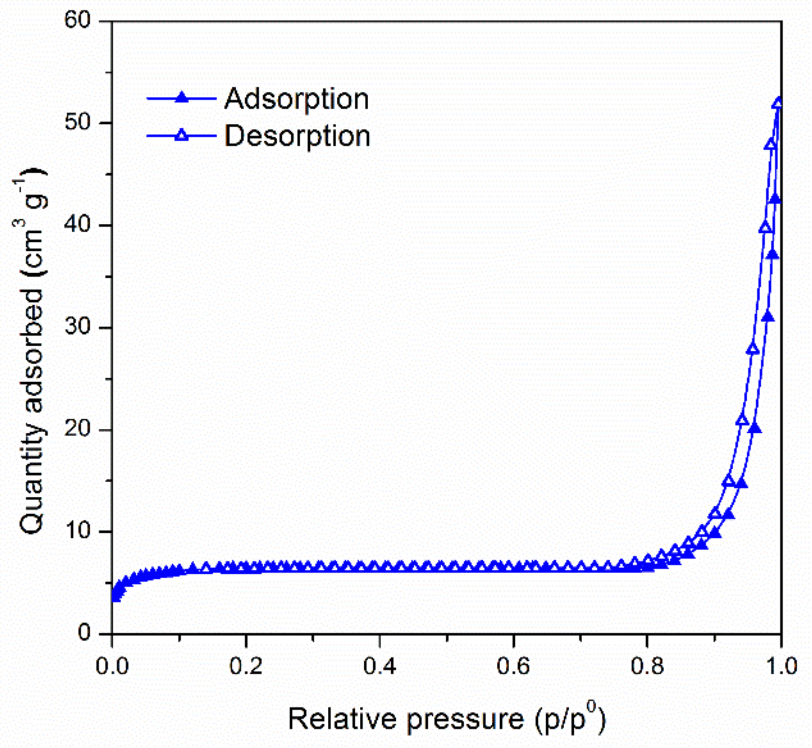

Figure S3. N_2 physisorption isotherm of unsupported porous multifaceted Pt NPs.

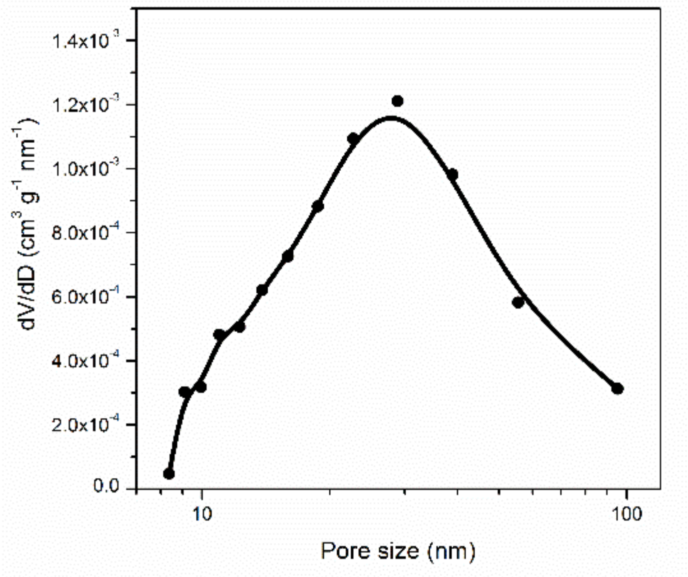

Figure S4. BJH pore size distribution of the unsupported porous multifaceted Pt NPs obtained from the desorption branch.

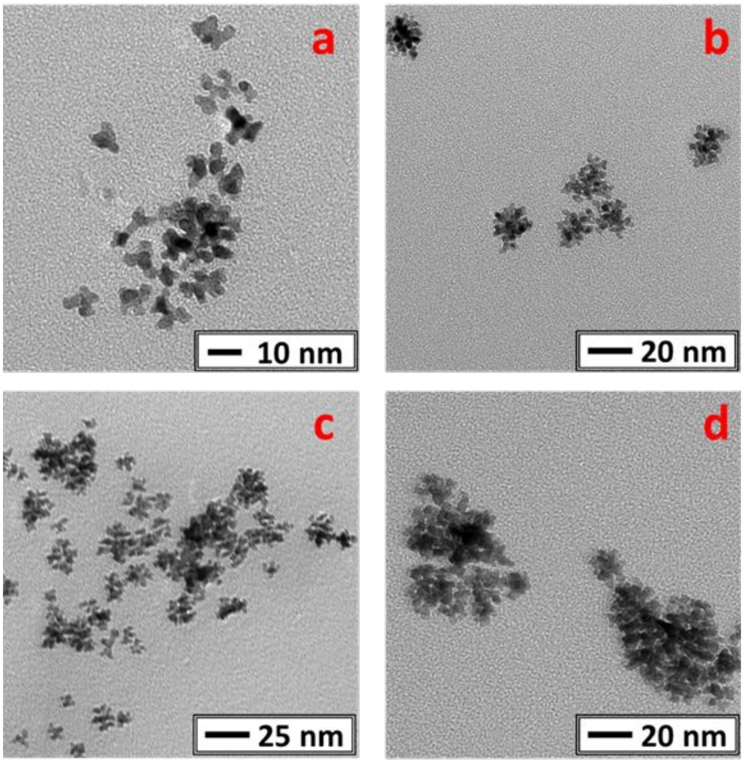

Figure S5. Representative TEM images of Pt NPs at 5 (a) and 10 (b) minutes after addition of OLAM then OLAC respectively (5 minutes after OLAM) at 120 °C and 5 (c) and 10 (d) minutes after addition of OLAC then OLAM respectively (5 minutes after OLAC).

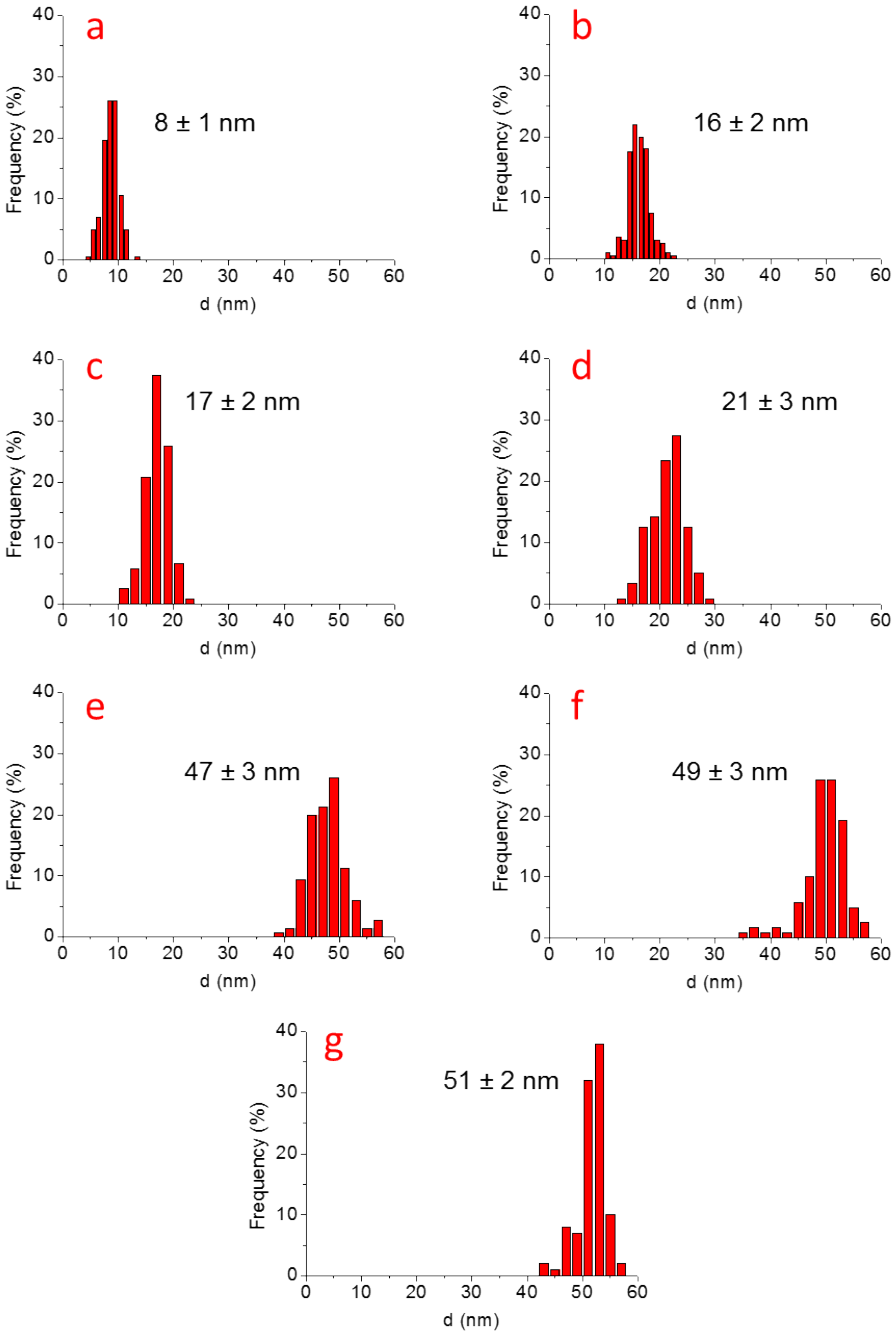

Figure S6. Dimensional analysis of the different Pt NPs at 5 min (a), 10 min (b), 15 min (c), 20 min (d), 30 min (e), 40 min (f) and 50 min (g) reaction time.

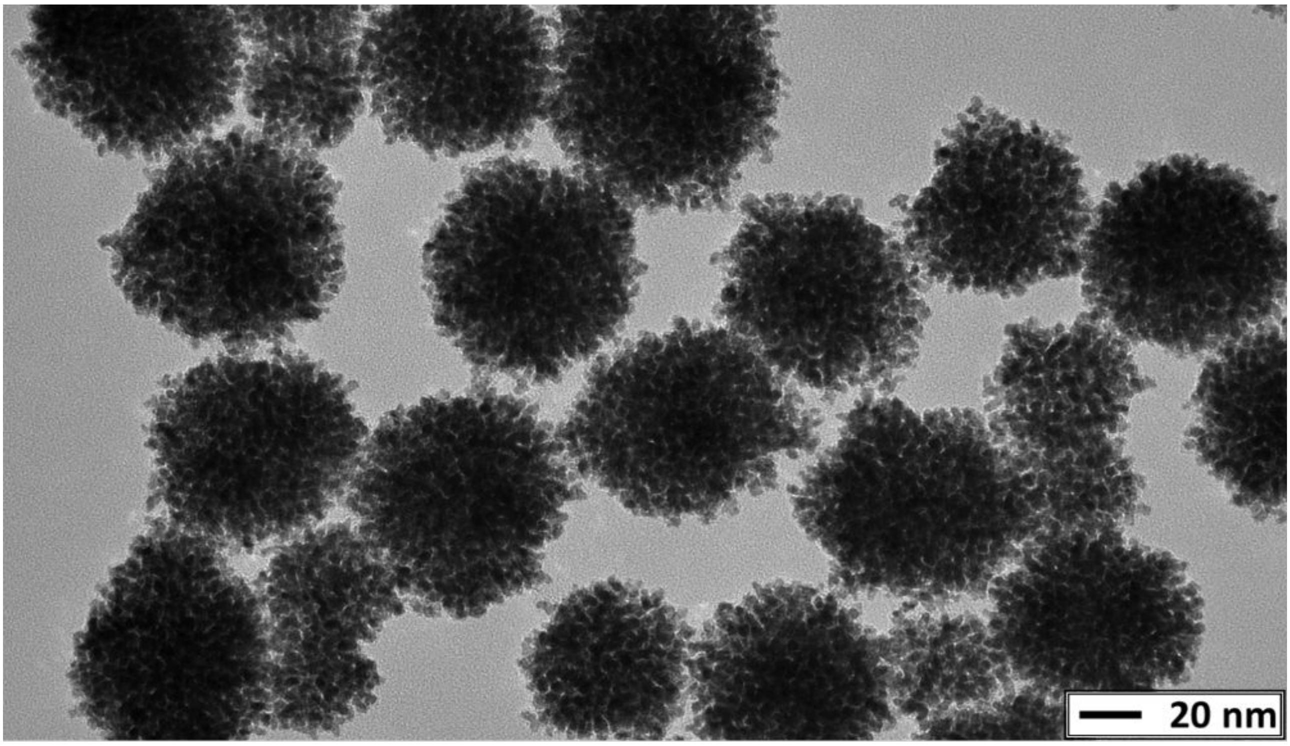

Figure S7. Representative TEM image of porous Pt NPs from the synthesis performed in air.

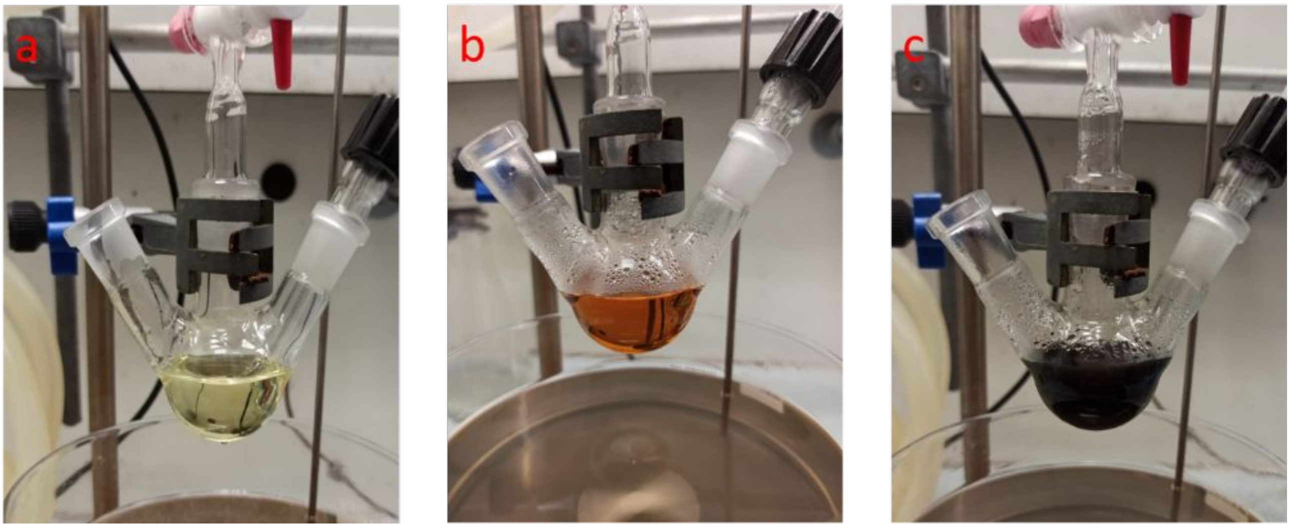

Figure S8. Reaction colour at room temperature (a), 180 °C for 1 h (b) and 200 °C for 1 h (c).

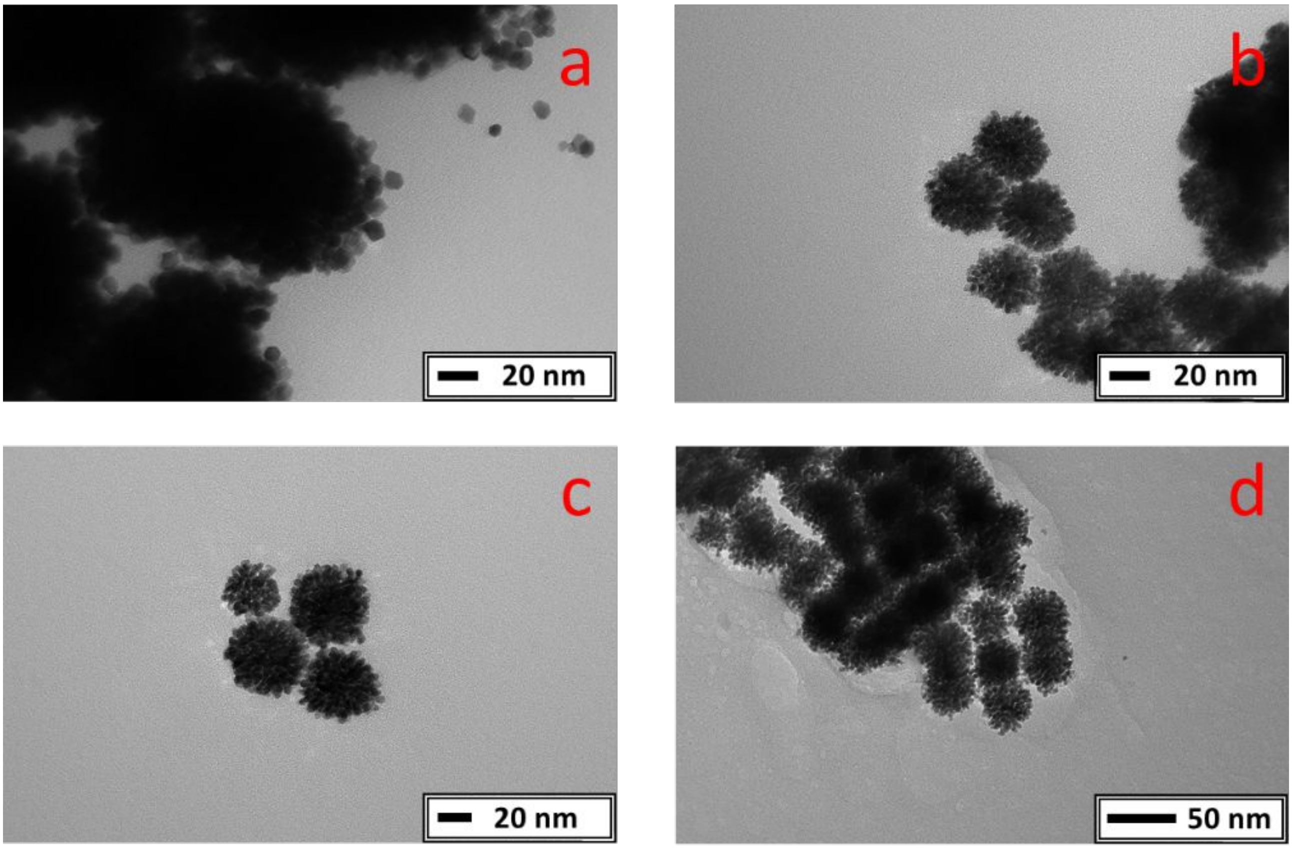

Figure S9. Representative TEM images of reaction performed with 1/3 (a), 1/1.5 (b), 1.5/1 (c) and 3/1 (d) OLAM/OLAC molar ratio.

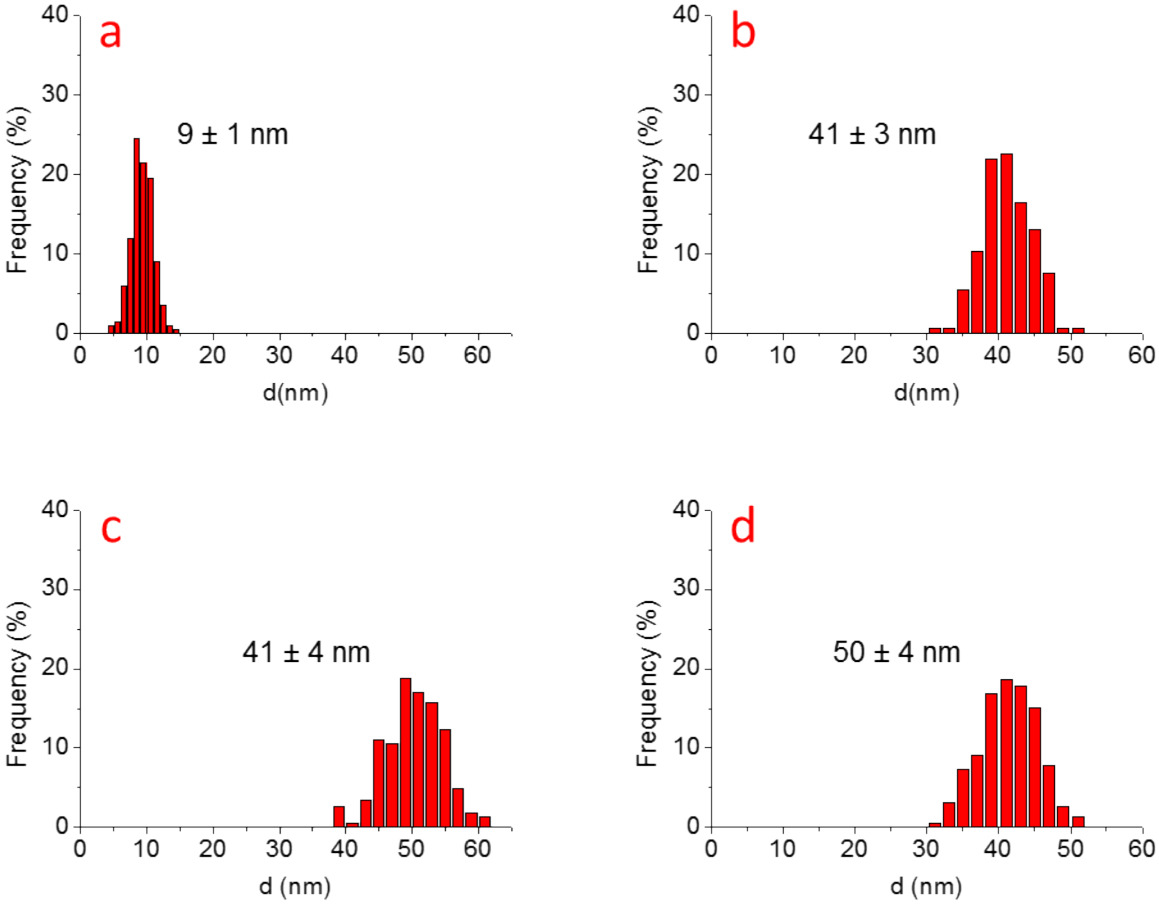

Figure S10. Dimensional analyses of Pt NPs obtained with different OLAM/OLAC molar ratios: 1/3 (a), 1/1.5 (b), 1.5/1 (c) and 3/1 (d).

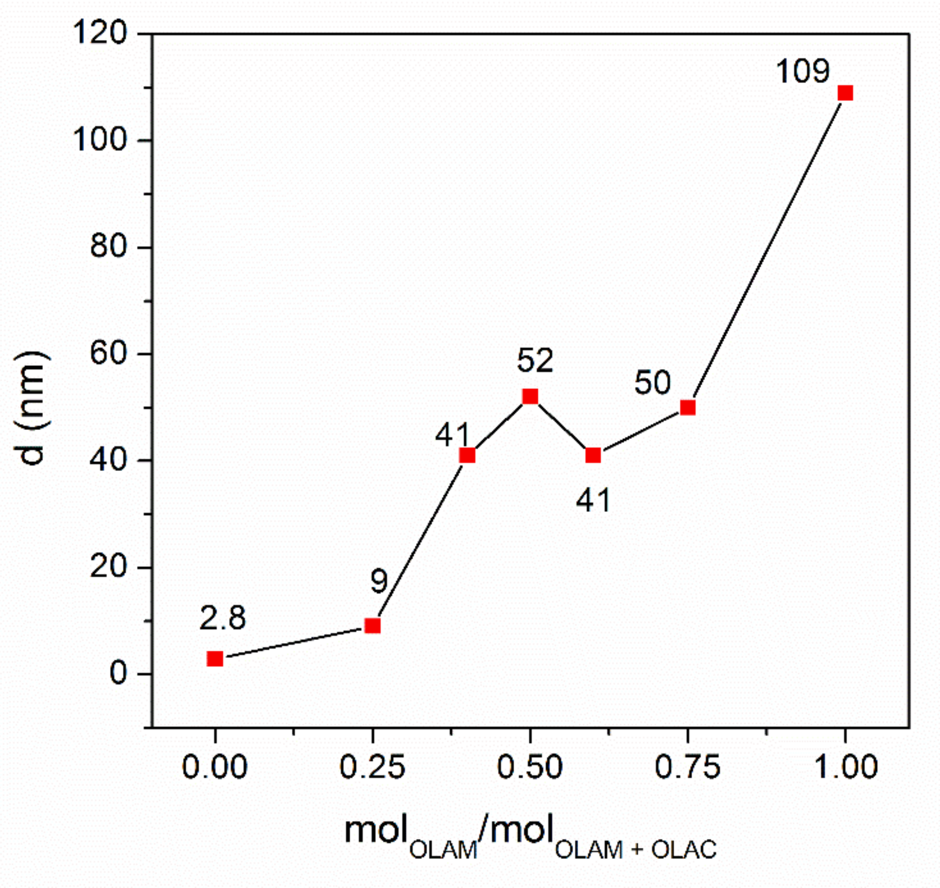

Figure S11. NPs dimension vs mol (OLAM) / mol (OLAM + OLAC) plot showing a proportional size increment with OLAM concentration.

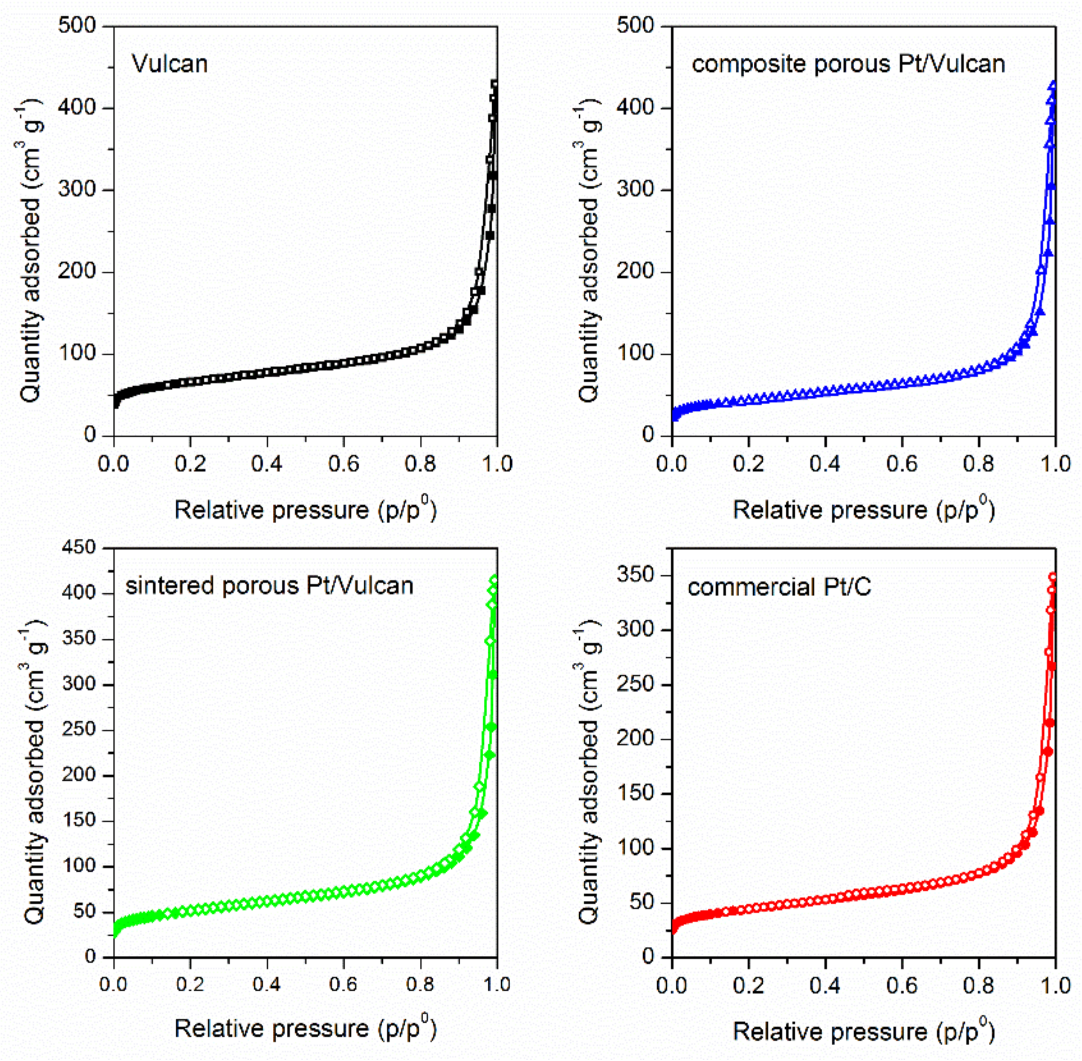

Figure S12. N_2 physisorption isotherms for Vulcan (black), composite porous Pt on Vulcan (blue), sintered porous Pt on Vulcan (green) and commercial Pt on carbon (red).

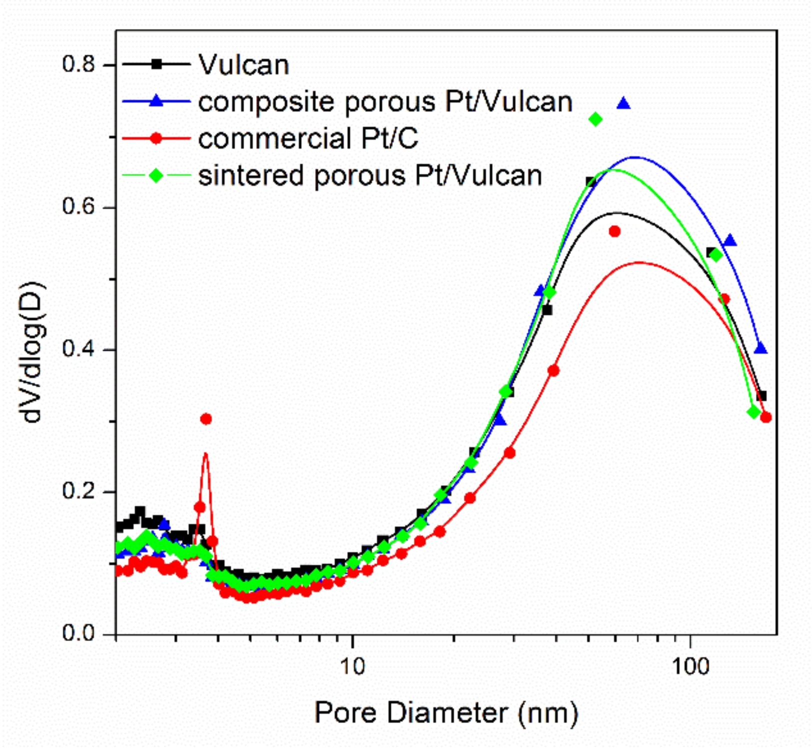

Figure S13. BJH pore size distribution for Vulcan (black), composite porous Pt on Vulcan (blue), sintered porous Pt on Vulcan (green) and commercial Pt on carbon (red).

Table S1. Summary of the textural properties of the investigated materials.

	S_{BET} [a] (m^2 g^{-1})	S_{ext} [b] (m^2 g^{-1})	S_{micro} [c] (m^2 g^{-1})	V_{tot} [d] (cm^3 g^{-1})	V_{micro} [e] (cm^3 g^{-1})	V_{meso} [f] (cm^3 g^{-1})	D_M [g] (nm)
Vulcan	200	146	54	0.604	0.036	0.568	51
composite porous Pt/Vulcan	140	125	15	0.627	0.012	0.615	63
comm. Pt/C	138	106	32	0.503	0.022	0.481	59
sintered porous Pt/Vulcan	140	113	27	0.525	0.019	0.506	53

[a] Specific surface area calculated following the BET method.

[b] Specific surface area external to micropores, determined from the t-plot analysis.

[c] Specific surface area of micropores.

[d] Total volume of pores calculated from BJH analysis.

[e] Total volume of micropores, determined from t-plot analysis.

[f] Total volume of mesopores.

[g] Maximum of the pore size distribution, determined by BJH analysis

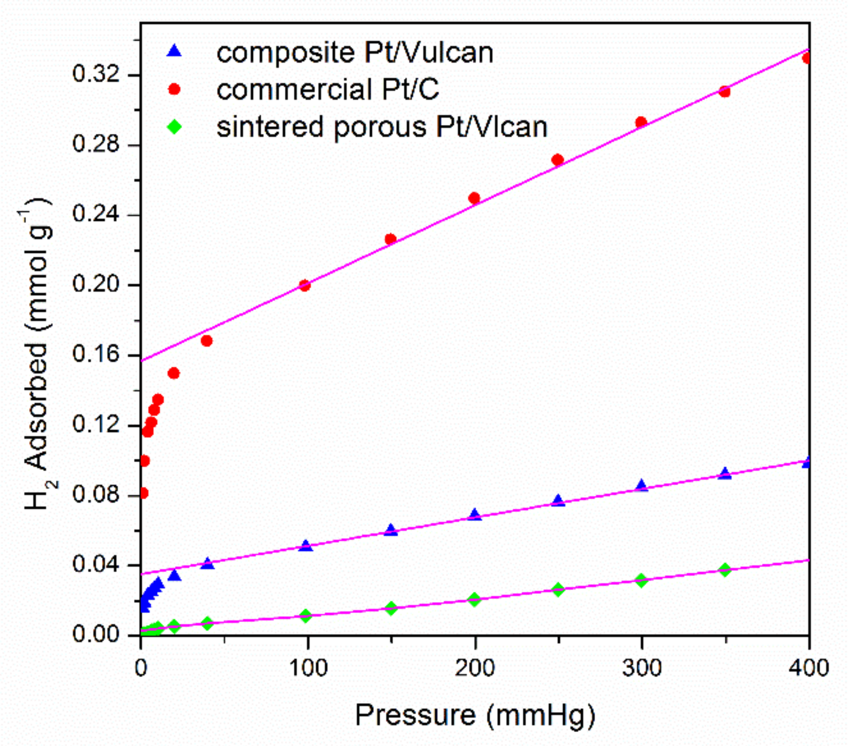

Figure S14. H_2 chemisorption measurements for porous multifaceted Pt on Vulcan and commercial Pt on carbon.

Table S2. Summary of the metal textural properties of the investigated materials.

	D % [a]	**d $_{part}$** [b] **(nm)**	**EMSA $_{cat}$** [c] **(m^2 g^{-1})**	**EMSA $_{Pt}$** [d] **(m^2 g^{-1})**
comm. Pt/C	23.9	5.0	11.8	59.1
composite porous Pt/Vulcan	7.3	15	2.7	18.1
sintered porous Pt/Vulcan	0.4	280	0.14	0.97

[a] Metal dispersion, calculated assuming a spherical shape of the metal particles.

[b] Apparent particle size.

[c] Exposed metal surface area (EMSA), expressed per quantity of catalyst.

[d] Exposed metal surface area (EMSA), expressed per quantity of platinum.

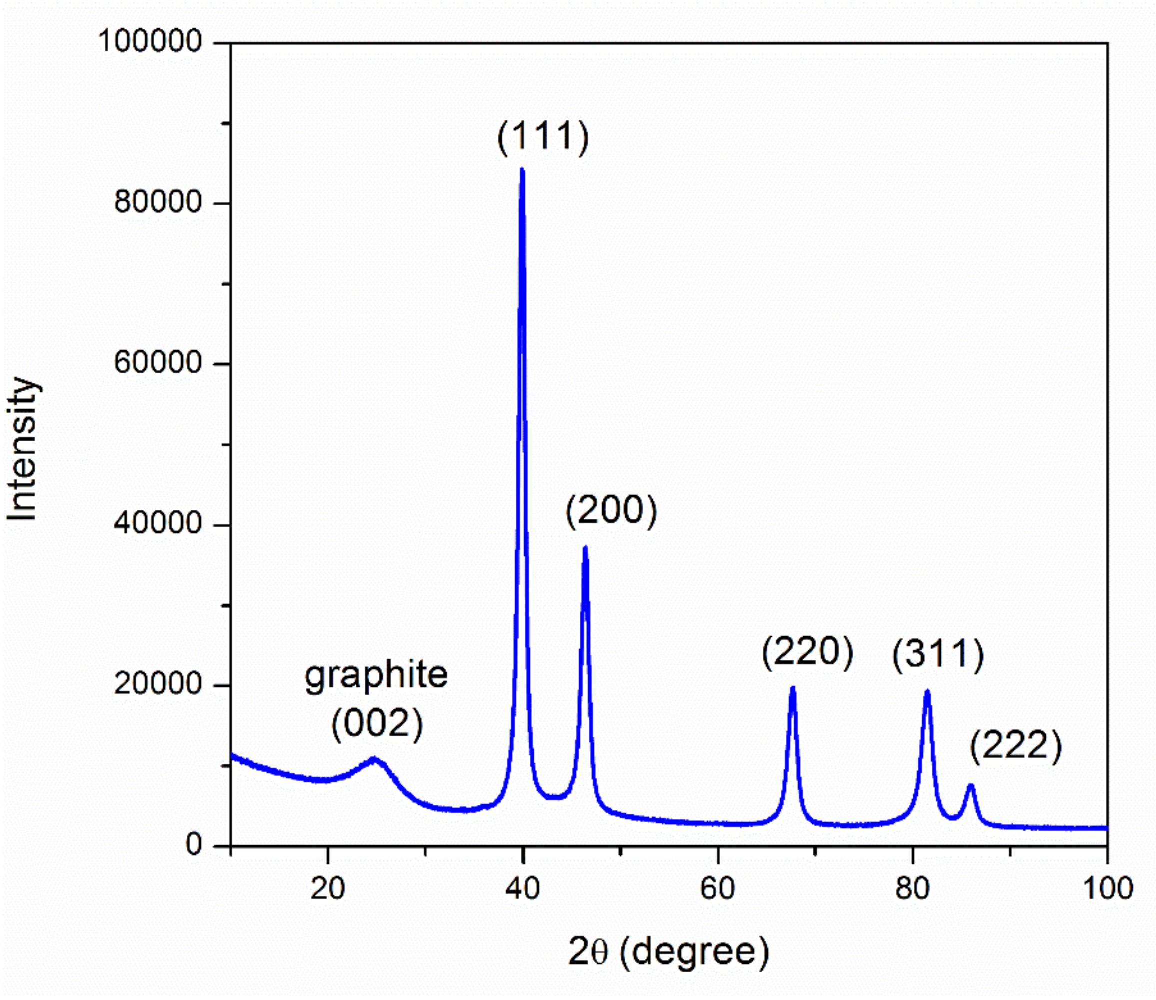

Figure S15. Powder x-ray diffraction pattern of the composite porous Pt NPs/Vulcan.

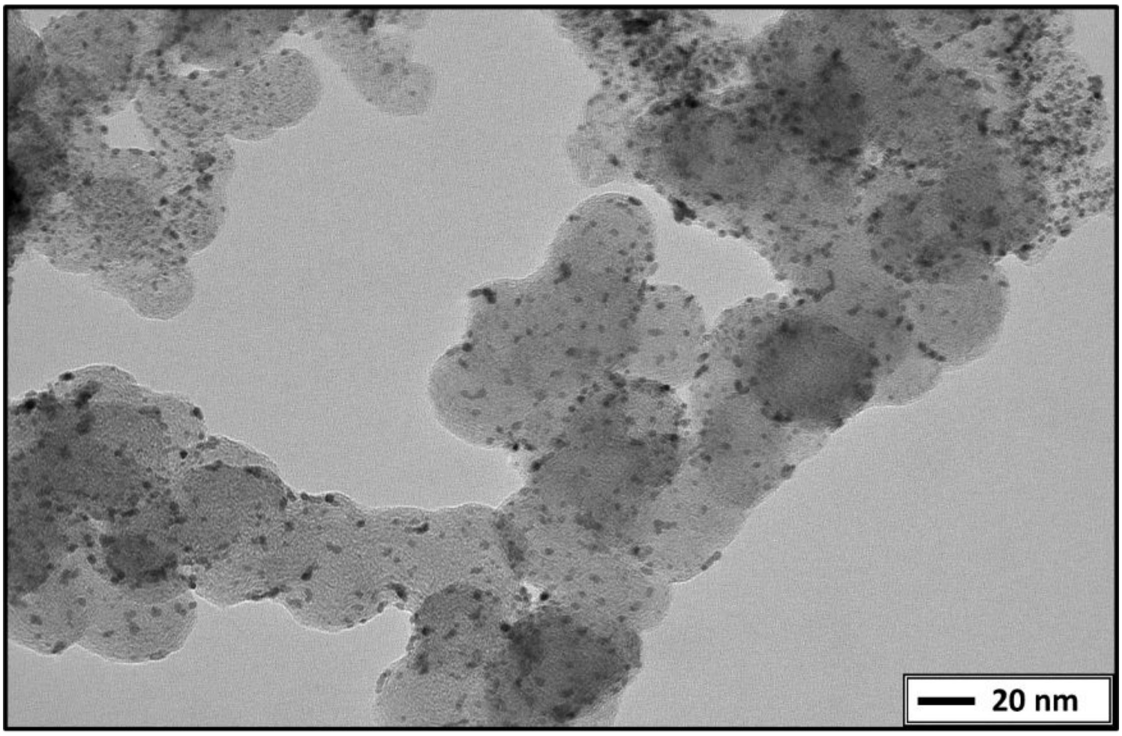

Figure S16. Representative TEM image of commercial platinum on carbon.

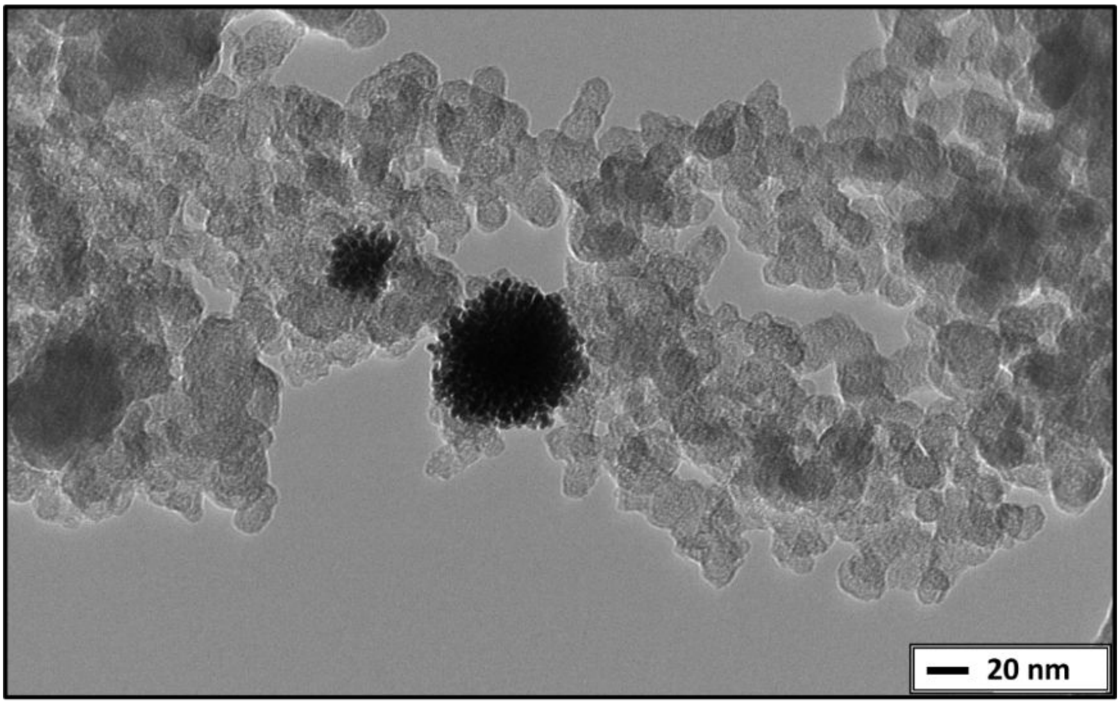

Figure S17. Representative TEM image of porous multifaceted Pt NPs deposited on Vulcan.

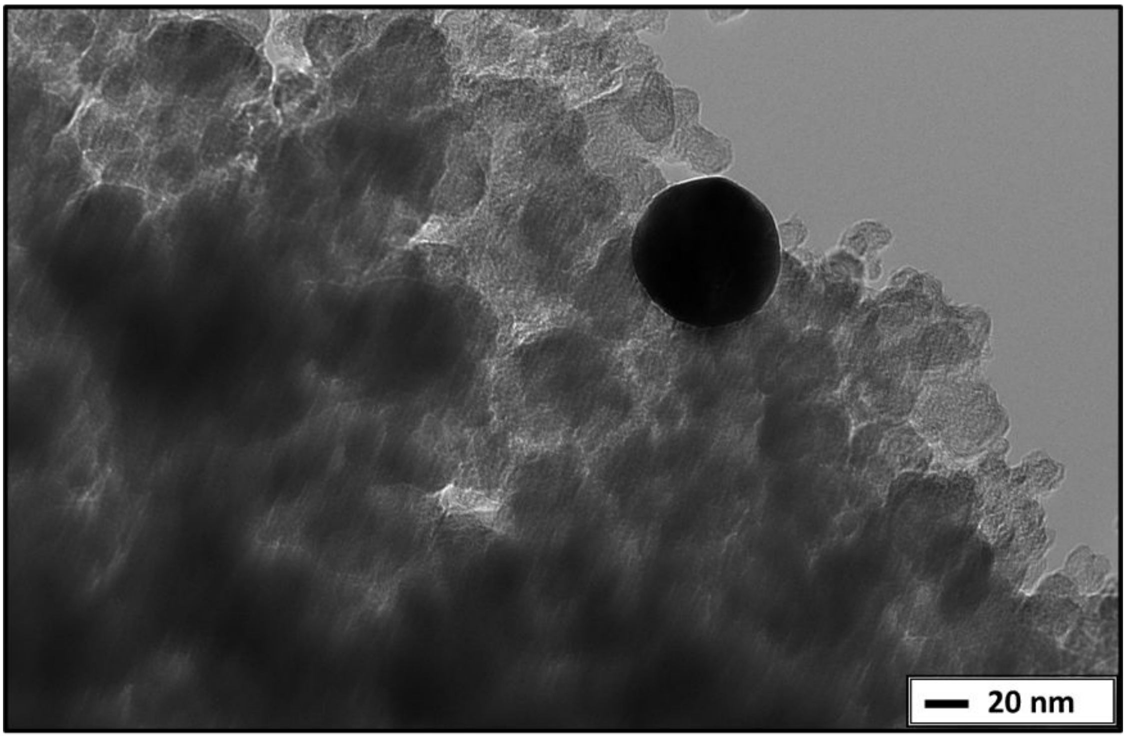

Figure S18. Representative TEM image of a sintered platinum NP on Vulcan.

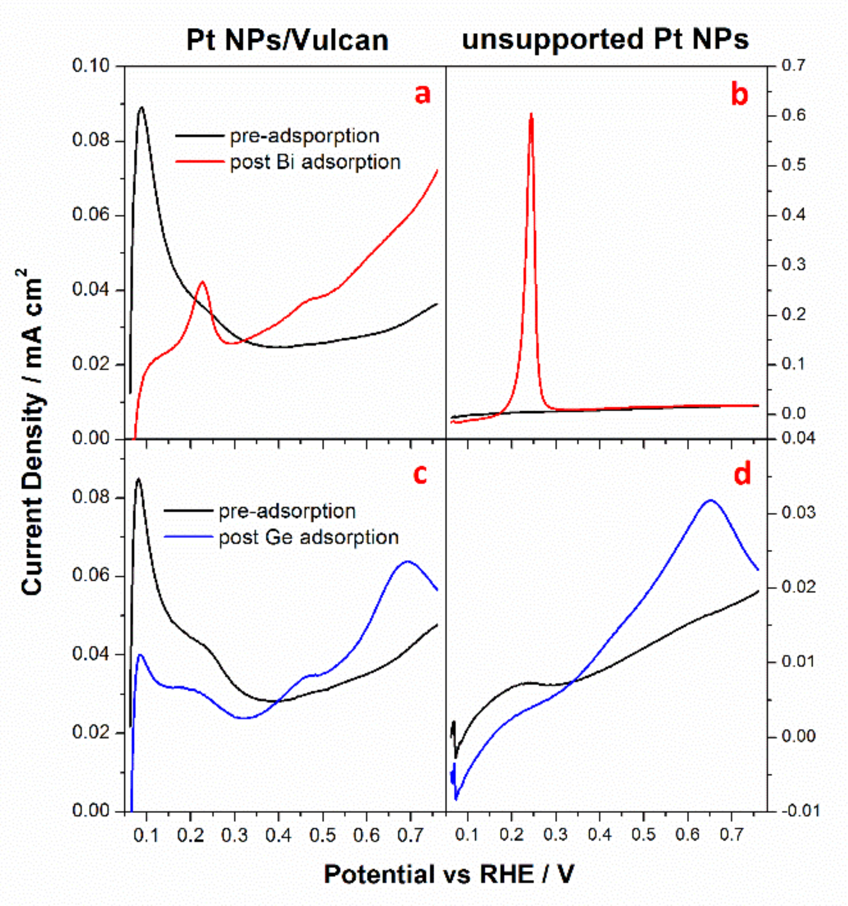

Figure S19. Voltammograms before/after Bi and Ge adsorption on porous multifaceted Pt NPs/Vulcan (a and c, respectively) and unsupported NPs (b and d, respectively). Measurements performed in 0.5 M H_2SO_4 at 20 mV s^{-1}.

Advanced Cleaning procedure for porous Pt NPs

Following an anonymous reviewer suggestion an advanced cleaning procedure was adopted before Bi adsorption experiments to investigate the possibility to better discriminate between the Pt surface sites. Specifically, after several washing steps with ethanol/n-hexane and centrifugation, the Pt NPs were dispersed in methanol and NaOH was added to the suspension. The suspension was first sonicated for 20 min to completely dissolve NaOH, then it was left to stir at room temperature for **two days**. By leaving the suspension to rest, a precipitate at the bottom is observed which is an indication of the ligand removal. The methanol/NaOH treated NPs were then washed with acetone and centrifuged, this step was repeated at least 3 times. A final washing step was performed with a mixture of acetone/water (3/1) after which the NPs were dried in vacuum at room temperature. We accurately checked the purity of all the reagents used for both the electrolyte (H_2SO_4) composition and the Pt NPs- based ink preparation, excluding Vulcan component to simplify the system under investigation. We removed the 2-propanol component in the standard ink recipe. However, Nafion 117 binder is necessary in the formulation of the ink and might represent a source of trace contamination. Different amounts of ink were also drop casted on the GC surface: 5, 14, 21 µL. Multiple CV cycles were substituted by CO-stripping treatment to clean the electrode surface. Different times of Bi-adsorption on the electrode surface (2-60 min) were investigated, according to the observations reported by Feliu and co-workers in Journal Power Sources 225 (2013) 323.

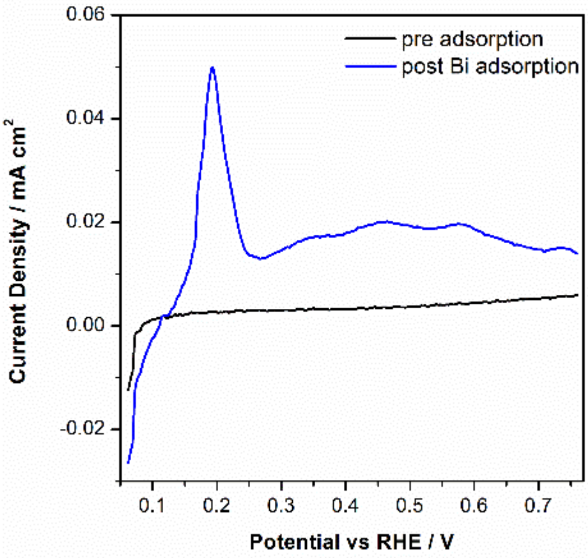

Figure S20. Voltammograms before/after Bi adsorption on porous multifaceted Pt NPs after the advanced cleaning treatment performed on a 5 µL drop casted electrode after 60 min contact time with bismuth oxide solution. Measurements performed in 0.5 M H_2SO_4 at 20 mV s.$^{-1}$

Figure S20 confirms the complexity of our Pt porous NPs with respect to single crystal, poly-oriented Pt electrodes and thin Pt films with preferential orientation, showing multi-peaks feature.

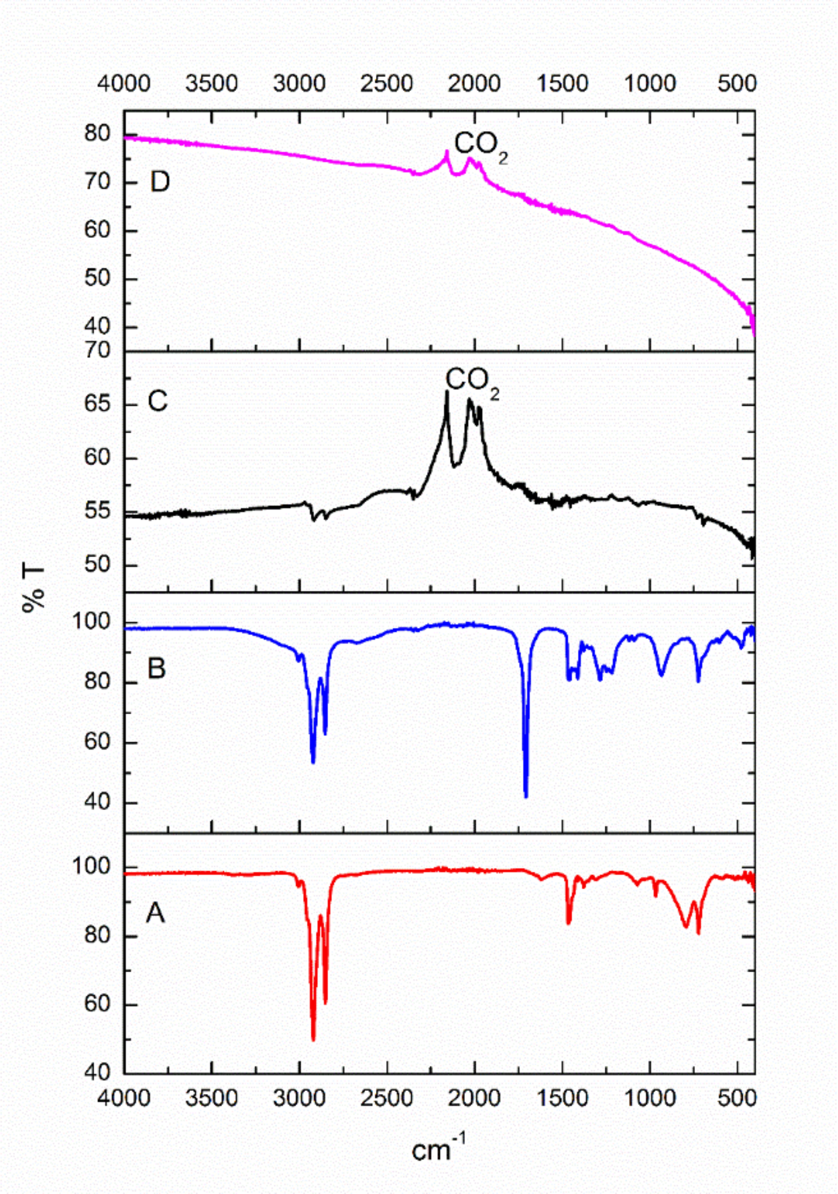

Figure S21. IR spectra of OLAM (a), OLAC (b), untreated Pt NPs (c) and NaOH treated Pt NPs (d).